Cellulose (2014) 21:4359–4368
DOI 10.1007/s10570-014-0453-6

ORIGINAL PAPER

Facile in situ synthesis of nickel/cellulose nanocomposites: mechanisms, properties and perspectives

C. H. Gong · X. X. Wang · H. J. Liu · C. Zhao · Y. D. Zhang · Y. S. Jia · H. J. Meng · J. W. Zhang · Z. J. Zhang

Received: 11 April 2014 / Accepted: 16 September 2014 / Published online: 25 September 2014

Abstract Nickel/cellulose nanocomposites with tunable magnetic behavior and electrical conductivity were fabricated by a facile in situ synthesis route with aqueous NaOH/urea solution as the solvent to dissolve and regenerate cellulose. It was found that Ni particles are uniformly dispersed in and immobilized by cellulose matrix, which indicates that regenerated cellulose fibers with coarse surface might act as templates to modulate the growth of Ni nanoparticles. Moreover, the size and morphology of Ni nanoparticles as well as the magnetic and conductive properties of Ni/cellulose nanocomposites is dependent on the concentration of Ni^{2+} in NaOH/urea aqueous solution. With an increase in the concentration of Ni^{2+} from 0.2 to 1.0 mol/L, the values of saturation magnetization increased from 16.6 to 38.5 emu/g, while the resistance decreased from 10^6 to 10^{-2} Ω cm. Particularly, multi-layer sample exhibits good absorption capacity and an additional effective bandwidth in the low-frequency region, showing promising potential as candidate electromagnetic functional fabric and cloth.

Keywords Nickel nanoparticles · Cellulose · Nanocomposite · Magnetic properties

Electronic supplementary material The online version of this article (doi:10.1007/s10570-014-0453-6) contains supplementary material, which is available to authorized users.

C. H. Gong · X. X. Wang · H. J. Liu · Y. D. Zhang · H. J. Meng
College of Chemistry and Chemical Engineering, Henan University, Kaifeng 475004, China

C. H. Gong (✉) · X. X. Wang · H. J. Liu · C. Zhao · Y. S. Jia · H. J. Meng · J. W. Zhang (✉) · Z. J. Zhang
Key Laboratory for Special Functional Materials of Ministry of Education, Henan University, Kaifeng 475004, China
e-mail: gong@henu.edu.cn

J. W. Zhang
e-mail: jwzhang@henu.edu.cn

Introduction

Recently, polymer nanocomposites containing metal nanoparticles have received increasing attentions due to their unique properties. Among abundant polymeric matrices, cellulose is a regrowing organic raw material with low cost. Particularly, cellulose fabrics with versatile functionalities could meet the requirements for tremendous applications (Jean et al. 2008; Klemm et al. 2005; Magalhães et al. 2009; Wotschadlo et al. 2013; Breitwieser et al. 2013).

cTwo basic clues are commonly applicable to fabricating cellulose-based composites. One is to incorporate metal nanoparticles into dissolved cellulose matrix (Rubacha 2006) mechanically, but this method is limited by the aggregation of nanoparticles. It is a challenge to reduce the aggregation of nanoparticles and control their assemblies at high concentrations. Another is to take advantage of the interactions

between surface-modified cellulose and metal nanoparticles to affording cellulose-based composites via in situ synthesis route. As a representative example of the second route, cellulose fibers with high surface coverage of metal nanoparticles could be preparated by the electrostatic interactions between negative charged cellulose and positive charged metal ions (Dong and Hinestroza 2009). Moreover, Cui and coworkers developed a solution-based technique to convert cotton textiles into conductive textiles by coating cellulose fibers with carbon nanotubes or graphene thin films. This route, however, is environmentally unfriendly due to the employment of organic surfactant for preparing CNT "ink" (Yu et al. 2011).

Recently, natural cellulose fibers with nanoporous surface features have been reported as substrates for the in situ synthesis of metal nanoparticles, because the functional surface group like hydroxyl and high microscopic porosity of natural cellulose fibers provide them with a preferable capability to form stable complexes with metal ions or act as confined reacting sites. This makes it feasible to directly in situ synthesize metal nanoparticles such as silver, copper, iron and cobalt nanoparticles (He et al. 2003; Yang et al. 2011). Besides, regenerated cellulose films with porous structure are not only templates but also useful supports for metal nanoparticles, which is significant for the in situ synthesis of cellulose nanocomposites containing magnetic nanoparticles such as Co_3O_4 (Liu et al. 2011) and plate-like Fe_2O_3 (Liu et al. 2006; Zhou et al. 2009). Such an approach, however, is applicable only to porous cellulose fibers. Therefore, it is imperative to design new applicable and facile techniques for scale-up production of functional textiles of both porous and nonporous cellulose fibers.

Previously we had successfully prepared Ni nanoparticles through the chemical reduction of Ni^{2+} by $N_2H_4{\cdot}H_2O$ in alkaline aqueous solution (Gong et al. 2008, 2010b). Considering that cellulose can be directly dissolved in alkaline aqueous solution of urea (Cai et al. 2004), we suppose that cellulose fibers in NaOH/urea aqueous solution could simultaneously act as the capping agents and spatially confined reacting sites of metal ions thereby more effectively controlling the aggregation and assemblies of target nanoparticles. In such a way, functional cellulose nanocomposites with a higher surface coverage than in bundled fibers could be afforded.

In the present research, therefore, we attempt to establish a new approach for preparing monodispersed Ni nanoparticles/cellulose nanocomposites, with which regenerated cellulose in NaOH/urea aqueous solution is adopted as the nanoreactor and the scaffold material as well. The influence of the concentration of precursor solution on the properties of as-prepared Ni/cellulose nanocomposites is also investigated. The facile one-pot friendly pathway, might favor not only promoting the fabrication of new functional cellulose nanocomposites and the development of spatially confined synthetic approaches but also acquiring additional understanding of the physicochemical processes occurring in a confined environment on sub-micrometer scale.

Experimental

Materials

All chemicals are analytical grade and were used without further purification. Medical absorbent cotton fiber was purchased from Union Health Materials Co. Ltd (Jiaozuo, China). Its viscosity-average molecular weight (M_η) was determined to be 1.03×10^5 by using an Ubbelohde viscometer in LiOH/urea aqueous solution at 25 ± 0.05 °C (Cai et al. 2006). Urea (CH_4N_2O), sodium hydrate (NaOH), nickel chloride ($NiCl_2{\cdot}6H_2O$), and hydrazine hydrate ($N_2H_4{\cdot}H_2O$, 80 %, mass fraction) were purchased from Kermel Chemical Co. Ltd (Tianjin, China).

Dissolution of cellulose

An appropriate amount of as-received cotton fiber was boiled in 17 % (mass fraction) NaOH solution for 2 h, followed by washing with distilled water until pH = 7. Resultant cotton fiber was dried in vacuum at 60 °C for 12 h and then dispersed in a pre-cooled (−14 °C) mixed solution of NaOH–urea–distilled water (mass ratio 8:12:80) under 10 min of vigorous stirring. Resultant mixture was stored in a refrigerator to afford dissolved cellulose, a colorless transparent solution, which is similar to the statements in many references (Cai et al. 2007a, b, 2008; Qi et al. 2009a).

Preparation of magnetic Ni/cellulose nanocomposites

An appropriate amount of $NiCl_2{\cdot}6H_2O$ was dissolved in distilled water. Resultant solution was added

dropwise to as-obtained colorless transparent cellulose solution under constant stirring. Into the mixed solution was then added dropwise an appropriate amount of 80 wt% $N_2H_4{\cdot}H_2O$ solution, followed by heating to 70 °C under continuous stirring yielding a dark flocculent product. The flocculent product was collected by filtration, rinsed thoroughly with water and ethanol, and dried in vacuum at 60 °C for 24 h affording desired Ni/cellulose nanocomposite. The cellulose fiber regenerated from as-received cotton fiber-NaOH/urea aqueous system is coded as RC, and the cellulose composite fibers (Ni/cellulose nanocomposites) regenerated from the aqueous solutions with 0.2, 0.5, and 1 M Ni^{2+} are coded as RC-0.2, RC-0.5, and RC-1.0, respectively, where the numeral suffixes refer to Ni^{2+} concentrations in the mixed cellulose reaction solutions. As an example, the reaction processes for preparing RC-0.5 are provided as supporting information (Figure S1).

Characterization

The phase composition and microstructure of as-synthesized Ni/cellulose nanocomposites were analyzed by means of X-ray diffraction (XRD; Philips X' Pert Pro X-ray diffractometer, Cu $K\alpha$ radiation, $\lambda = 0.15418$ nm), Fourier transform infrared spectrometry (FT-IR; AVATAR360, NicoletIn-Strument Corrp), scanning electron microscopy (SEM; JEOL JSM-5600LV scanning electron microscope, acceleration voltage 20 kV) and transmission electron microscopy (TEM; JEOL JEM-2100 transmission electron microscope, accelerating voltage 200 kV). The main constituent elements of sample RC-0.5 were determined by means of energy-dispersive X-ray spectrometry (EDS) attached to the SEM. Thermal gravimetric analysis (TGA) was conducted with a thermogravimetric analyzer (Mettle-Toledo, SDTA851e); and 5 mg of to-be-tested Ni/cellulose nanocomposites was cut into powder, placed in an aluminum oxide crucible, and heated from 20 to 700 °C at a rate of 10 K/min in air atmosphere. Magnetic measurements were conducted with a vibrating sample magnetometer (VSM, Lake Shore 7400). A digital milliohm meter (Model YF-508, 0–20 KΩ, Yu Fong Electric Co., Ltd., Taiwan, China) was used to measure the resistance values of the Ni/cellulose nanocomposites, making use of Kelvin (4-wire) resistance measurement technique. Moreover, the films of Ni/cellulose nanocomposites obtained after filtration were cut into square pieces with a size of 200 mm × 200 mm and used for microwave absorption test. The reflection loss versus frequency of as-prepared absorbers was measured with an HP8720B vector network analyzer and standard horn antennas in an anechoic chamber at a testing frequency range of 2–18 GHz (Wang et al. 2008).

Results and discussion

The XRD patterns of as-received cotton fiber and regenerated cellulose fiber RC as well as Ni/cellulose nanocomposites RC-0.2, RC-0.5, and RC-1.0 are shown in Fig. 1a. As-received cotton fiber shows a broad weak peak between 14° and 17° and a sharp diffraction peak at $2\theta = 22.7°$, assigned to the typical diffraction pattern of cellulose I structure (Qi et al. 2009b). Regenerated RC shows broad diffraction peaks around $2\theta = 12.1°$, 20.3°, and 22.2° for (1–10), (110), and (020) planes are assigned to cellulose II crystal, which indicates that treatment of as-received cellulose fiber in NaOH solution causes structural transformation from cellulose I to cellulose II (Nishiyama et al. 2002; Langan et al. 2001; Nishiyama et al. 2012; French and Santiago Cintrón 2013; French 2014).

In the meantime, RC-0.2, RC-0.5, and RC-1.0 retain the diffraction peaks of crystal cellulose II, while they show three characteristic peaks of face-centered cubic Ni ((111), (200), and (220) crystal planes) at 45.1°, 52.4°, and 76.5° (Gong et al. 2010a). Besides, the XRD pattern shows obvious signs of broadening, indicating that the as-prepared Ni sample may consist of nanocrystallites. The average crystalline size of Ni nanoparticles in RC-0.2, RC-0.5, and RC-1.0 has been calculated based on the Scherer equation, and the value is 16, 13.7 and 13.3 nm, respectively, which means that the Ni^{2+} concentration has a very little influence on the crystalline size of Ni nanoparticles. Moreover, a typical selected area electron diffraction (SAED) pattern obtained along a typical individual Ni nanoparticle in RC-0.5 is displayed in Figure S2. The four fringe patterns can be indexed as (111), (200), (220), (311) of pure face-centered cubic (fcc) nickel, indicating that the nickel nanoparticles in this case had polycrystalline structure, which corresponds well to the XRD pattern. The main constituent elements of RC-0.5 were determined by EDS and the results were shown in Figure S3, which indicated the existing of "Ni" in the magnetic Ni/cellulose nanocomposites (Fig. 2).

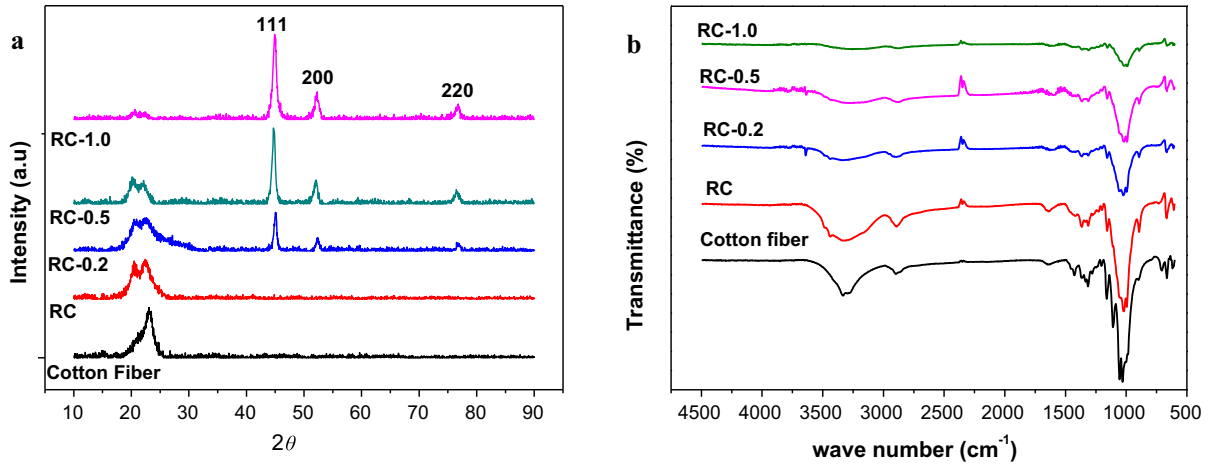

Fig. 1 XRD patterns (**a**) and FT-IR spectra (**b**) of as-received cotton fiber and regenerated cellulose fiber RC as well as Ni/cellulose nanocomposites RC-0.2, RC-0.5, and RC-1.0

Furthermore, the relative intensity of the diffraction peaks of Ni nanoparticles increases with increasing concentration of precursor, which indicates that the nanophase loading on the cellulose matrix increases therewith. Moreover, it could be found that the relative intensity of the diffraction peaks of cellulose decreases with increasing content of Ni nanoparticles concentration, which indicates the crystallinity of cellulose in RC-0.2, RC-0.5, and RC-1.0, is apparently lower than that in RC fiber, and it decreases with increasing content of Ni nanoparticles (Donia et al. 2012). Thus it can be inferred that the formation and incorporation of Ni nanoparticles leads to destruction of the crystallinity of cellulose in as-prepared Ni/cellulose nanocomposites to some extent.

The FT-IR spectra of as-received cotton fiber and regenerated cellulose fiber RC as well as Ni/cellulose nanocomposites RC-0.2, RC-0.5, and RC-1.0 are displayed in Fig. 1b. As-received cotton fiber shows an absorption band of cellulose I crystal at 1,100 cm^{-1}, but this absorption band is absent for regenerated cellulose fiber RC and Ni/cellulose nanocomposites RC-0.2, RC-0.5, and RC-1.0. This further confirms that regenerated cellulose fibers undergo crystal structure transformation from cellulose I to cellulose II (Kondo and Sawatari 1996), which is in good agreement with relevant XRD data. Ni^{2+} ions could be bound to cellulose macromolecules probably via electrostatic interactions, because the electron-rich oxygen atoms of polar hydroxyl and ether groups of cellulose are expected to interact with electropositive transition metal cations. Besides, the stretching vibration bands of the hydroxyl groups of cellulose at 3,300–3,500 cm^{-1} is shifted towards higher wave numbers and become broader and weaker with increasing Ni^{2+} concentration, which indicates that there exists a strong hydrogen bonding interaction between the hydroxyl group of cellulose and Ni nanoparticles (Kondo and Sawatari 1996; Schwanninger et al. 2004).

As shown in Figure S1a, when as-received cotton fiber is immersed in NaOH/urea aqueous solution precooled to −14 °C, the hydrogen-bonded network structure between the cellulose macromolecules and small molecules in the solvent is created rapidly to form an inclusion complex, bringing cellulose into the aqueous solution. The cellulose solution is relatively unstable and can be very sensitive to temperature, polymer concentration and storage time, leading to the aggregations (Cai et al. 2008; Qi et al. 2008; Li et al. 2012).

To determine the state of the cellulose fiber matrix and incorporated Ni nanoparticles, we conducted optical microscopic analysis and SEM analysis. When the temperature increases, the network structure was destroyed, and the dissolve degree of cellulose fiber increase too. For example, when the cellulose solution reaction system is kept at a temperature of as high as 70 °C, swelled cellulose gels with a diameter of ~30 μm are formed, which is attributed to the strong self-affinity of cellulose in association with the destruction of the inclusion complex. The regenerated

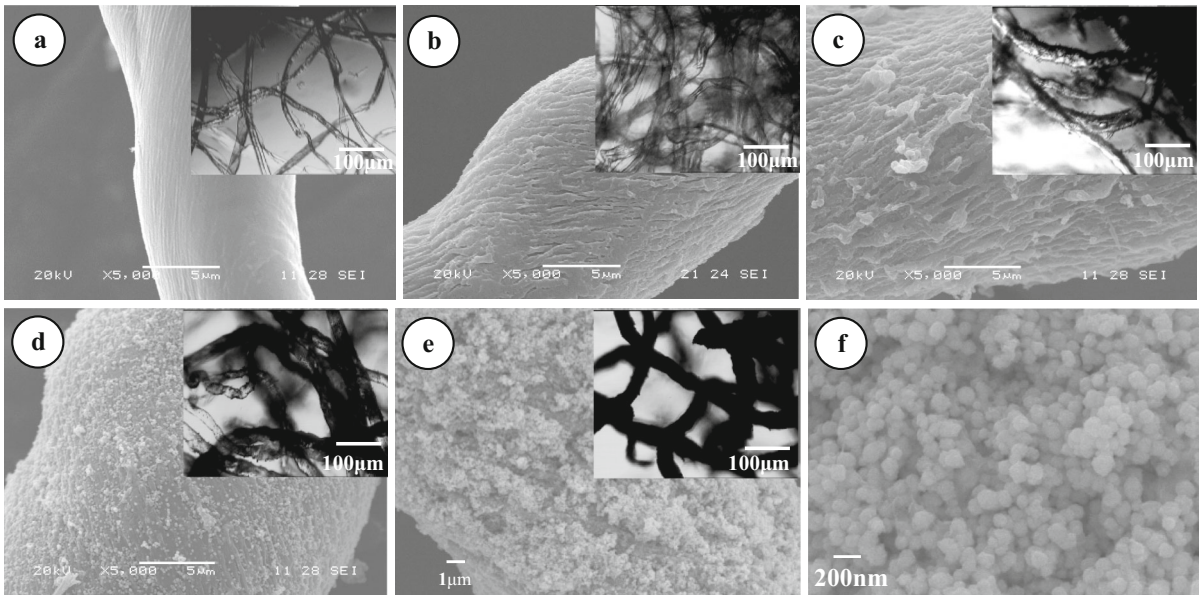

Fig. 2 SEM morphology of as-received cotton fiber (**a**) and regenerated cellulose fiber RC (**b**) as well as as-prepared Ni/cellulose nanocomposites RC-0.2 (**c**), RC-0.5 (**d**), and RC-1.0 (**e**). The *upper right insets* show the corresponding optical microscopic images of the samples and (**f**) is the higher magnification image of RC-1.0

cellulose fibers in this reaction system were expected as the nanoreactor of the reduction of Ni^{2+} ions, which could control the aggregation and assemblies of target Ni nanoparticles effectively. Resultly, a dark flocculent product, the desired magnetic Ni/cellulose nanocomposite can be successfully synthesized. The mechanism scheme for preparing Ni/cellulose nanocomposite was shown in Figure S4. Furthermore, as-received cotton fiber has a smooth surface, while the regenerated cellulose fiber and as-prepared Ni/cellulose nanocomposites exhibit a rough surface morphology. In combination with the XRD and FT-IR data, we can conclude that the regeneration treating in alkaline solution brings not only structure change but also morphology change of the cotton fibers.

Corresponding optical microscopic pictures of as-received cotton fiber and regenerated cellulose fiber RC as well as as-prepared Ni/cellulose nanocomposites RC-0.2, RC-0.5, and RC-1.0 are shown in Figure S5. It is clearly seen that the color of the fiber samples changes from white to grey and then to black with an increase of the concentration of Ni^{2+} from 0.0 to 1.0 M, which means that the increase of nickel concentration in the cellulose solution reaction system triggers the increase of content of magnetic Ni nanoparticles in as-prepared Ni/cellulose nanocomposites.

To further examine the effect of Ni^{2+} concentration in cellulose solution reaction system on the size and morphology of Ni nanoparticles in as-prepared Ni/cellulose nanocomposites, we dissolved as-prepared nanocomposites in NaOH/urea aqueous solution and collected magnetic Ni nanoparticles with the assistance of magnetic separation. Resultant Ni nanoparticles were washed with ethanol for several times and then dispersed in ethanol. A few drops of as-dispersed Ni nanoparticles were finally introduced onto carbon-coated copper grids and allowed to evaporate in air at room temperature thereby providing samples for TEM analysis. Figure 3 shows the TEM images of Ni nanoparticles collected from nanocomposites RC-0.2, RC-0.5, and RC-1.0. It is seen that the Ni nanoparticles collected from nanocomposite RC-0.2 exhibit rod-like and plate-like morphology; the rod-like nanoparticles have an average length of about 50 nm and a diameter of about 3–5 nm, and the plate-like nanoparticles have a diameter of 50 nm, which was close to the length of the rod-like nanoparticles. Therefore it could be concluded that the nanoparticles were plate-like with a length about 50 nm and thickness of 3–5 nm. When Ni^{2+} ion concentration increases from 0.2 to 1.0 M, it could be found that the average length of incorporated Ni nanoparticles increases from 50 to 130 nm, and

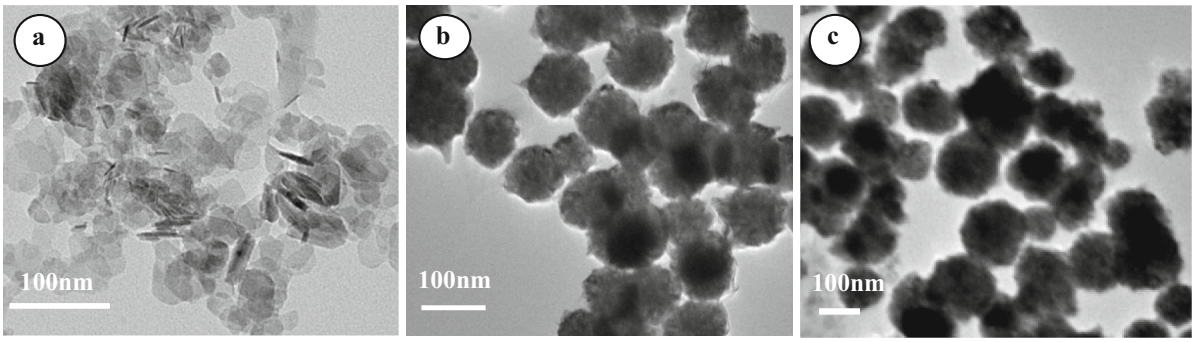

Fig. 3 TEM images of Ni nanoparticles in RC-0.2 (**a**), RC-0.5 (**b**), and RC-1.0 (**c**)

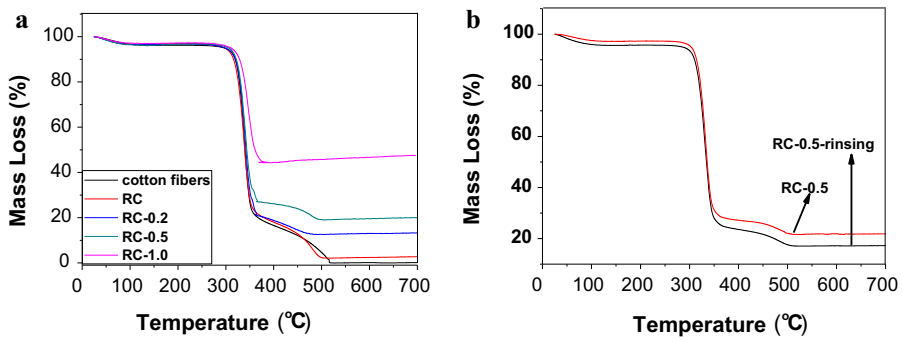

Fig. 4 Weight loss as a function of temperature for RC fibers and various as-prepared Ni/cellulose nanocomposites (**a**), weight loss of RC-0.5 before and after rinsing (**b**)

their thickness also increases therewith. Moreover, Ni nanoparticles in three kinds of as-prepared Ni/cellulose nanocomposites have a relatively narrow size distribution. In combination with the abovementioned structure and morphology of as-prepared Ni/cellulose nanocomposites, we can infer that the pores (ether and crevice) in association with the high oxygen content and hydroxyl density of the cellulose matrix would lower the mobility of Ni^{2+} ions, enhance the formation of nickel nuclei, and prevent the growth of larger particles. This is particularly true at low Ni^{2+} ions concentrations, and explains formation of monodisperse Ni nanoparticles under such conditions. At higher Ni^{2+} ions concentrations, larger amounts of Ni^{2+} ions are adsorbed on cellulose fibers, leading to large and widely distributed particles after reduction. As a result, the surface of regenerated cellulose fibers is uniformly covered by fine monodispersed Ni nanoparticles.

The weight loss versus temperature curves of as-received cotton fiber and various regenerated cellulose fibers (Ni/cellulose nanocomposites) are shown in Fig. 4. All tested samples undergo a small weight loss of about 8–11 % around 80 °C, which is due to the release of moisture upon heating. As the temperature further rises, all tested cellulose fibers undego two-step of noticeable weight loss: the weight loss in the temperature range of 300–380 °C is ascribed to the onset of cellulose decomposition, and that within 420–540 °C is attributed to the decomposition of cellulose. Moreover, the content of Ni nanoparticles on cellulose fibers increases rapidly from 13.3 to 43.6 wt% when the concentration of $NiCl_2$ rises from 0.2 to 1.0 M, which could be attributed to the diffusion equilibrium of Ni^{2+} between the $NiCl_2$ solution and cellulose matrix. In other words, higher concentration of $NiCl_2$ leads to higher content of Ni nanoparticles in as-prepared Ni/cellulose nanocomposites, as evidenced by relevant SEM analysis and XRD analysis.

The stability of Ni nanoparticles in cellulose fibers is very important to the properties of the composite fibers. Here, RC-0.5 was taken as a sample to investigate the dispersion stability of the Ni-NPs in the cellulose fibers by the help of TG. Firstly, in a 100 ml beaker, 5 g RC-0.5 were dispersed in 50 ml distilled water. Then, the beaker was ultrasonically treated at a power of 100 W (KQ-218, Kunshan Ultrasonic Instruments Co., Ltd., China) for 30 min

(the distilled water in the beaker was replaced every 5 min). Rinsing by distilled water could effectively remove those Ni-NPs that were not anchored to cellulose fibers tightly. As shown in Fig. 4b, it could be found that after they have been ultrasonically treated for 30 min, the content of Ni nanoparticles in cellulose fibers decreases from 19.9 to 17.4 wt%. This stabilization of Ni metal in the magnetic Ni/cellulose nanocomposites probably arises from the strong interaction between Ni^{2+} ions and the hydroxyl and ether groups of cellulose macromolecule. The ether and hydroxyl functions not only anchor the metal ions tightly onto the fibers via ion–dipole interactions, but also after reduction stabilizes the as prepared nanoparticles via surface interactions, which is beneficial for their application in textiles field (He et al. 2003; El-Shishtawy et al. 2011).

Figure 5a shows the magnetic properties of Ni/cellulose nanocomposites with different Ni contents measured by VSM at room temperature. On the one hand, as indicated by the magnetization hysteresis hoops, all as-synthesized Ni/cellulose nanocomposites show typical ferromagnetic behavior; and their magnetic properties tend to highly depend on Ni content. Namely, the saturation magnetization of Ni/cellulose nanocomposites tends to increase with increasing Ni content, and nanocomposites RC-0.2, RC-0.5, and RC-1.0 have a saturation magnetization (*Ms*) of 16.6, 31.8, and 38.5 emu/g, respectively. Such an increase in the saturation magnetization of Ni/cellulose nanocomposites with elevating Ni content can be well understood if one notices that cellulose is nonmagnetic but Ni nanoparticles are magnetic. Moreover, the *Ms* of as-prepared Ni/cellulose nanocompsoites is generally lower than that of bulk Ni (*Ms* = 54–55 emu/g), which is because the spin disorder on the surface of Ni nanoparticles significantly reduces the total magnetic moment (Gong et al. 2010a). In combination with relevant TEM images, we can further infer that the decrease of *Ms* values with decreasing particle size from RC-1.0 to RC-0.2 may also be partly attributed to the reduced magnetization on the surfaces of Ni nanoparticles.

On the other hand, the coercivity (*Hc*) values of various as-prepared Ni/cellulose nanocomposites tend to rise with decreasing Ni nanoparticle content. Namely, as-prepared Ni/cellulose nanocomposites obtained at Ni^{2+} concentrations of 0.2, 0.5, and 1 exhibit *Hc* values of 201 Oe, 150 Oe, and 101 Oe, and they are higher than 100 Oe, that of bulk nickel. It is well known that the magnetic properties of magnetic materials are related to the crystallite size, structure and shape, and the shape of the hysteresis loop is strongly dependent on the specific surface area of particles and the magnetic anisotropy (Gong et al. 2009; Shafi et al. 1998; Zhang et al. 2006). In the present research, the *Hc* values of as-prepared Ni/cellulose nanocomposites tend to decrease with increasing Ni^{2+} concentration, possibly because plate-like Ni particles in RC-0.2 have higher shape anisotropy and lower size than the counterparts in RC-0.5 and RC-1.0 (the relationship between the coercivity and particle size (*D*) can be described as $Hc = a + b/D$; *D* is particle size, and a and b are constants) (Gong et al. 2014). This conforms well to what have been reported elsewhere in that the samples with higher shape anisotropy and smaller particle size have higher coercivity (Jia et al. 2008; Soumare et al. 2008; Wang et al. 2009).

The volume resistivity values of the samples were calculated using the following equation:

$$\rho_v = R \times \delta \times d/L(\Omega\ \mathrm{cm}) \quad (1)$$

where ρ_v is the volume resistance of the sample (Ω cm), *R* is the resistance value of the sample (Ω), δ is the thickness of the sample (cm), *d* is the width of the sample (cm), and *L* is the effective length of the sample (cm). Understandability, both the initial cotton fibers and RC without Ni combined had a very high resistivity beyond the scale of the instrument ($>10^6$ Ω). Apparently, the conductivity of Ni/Cellulose nanocomposites increases sharply with the increase of the content of the nickel, and the calculated volume resistivity (Ω cm) values of RC-0.2, RC-0.5, and RC-1.0 is 1.15×10^6, 3.36×10^2 and 1.21×10^{-2} Ω cm, respectively. The logarithmic volume resistivity (Ω cm) of the cellulose based composite samples are shown in Fig. 5b. When combined with the results of SEM and TG, it could be found that, in this work, due to the small size and dispensability of the nickel powders on the surface of the cellulose, the conductive networks could be formed via the contact and interlocking of the conductive particles. Thus, though the content of conductive filler is very low, the conductive is very high when compared with the results in other investigation (Gong et al. 2008). Moreover, the low content of nickel means low density and low cost of the

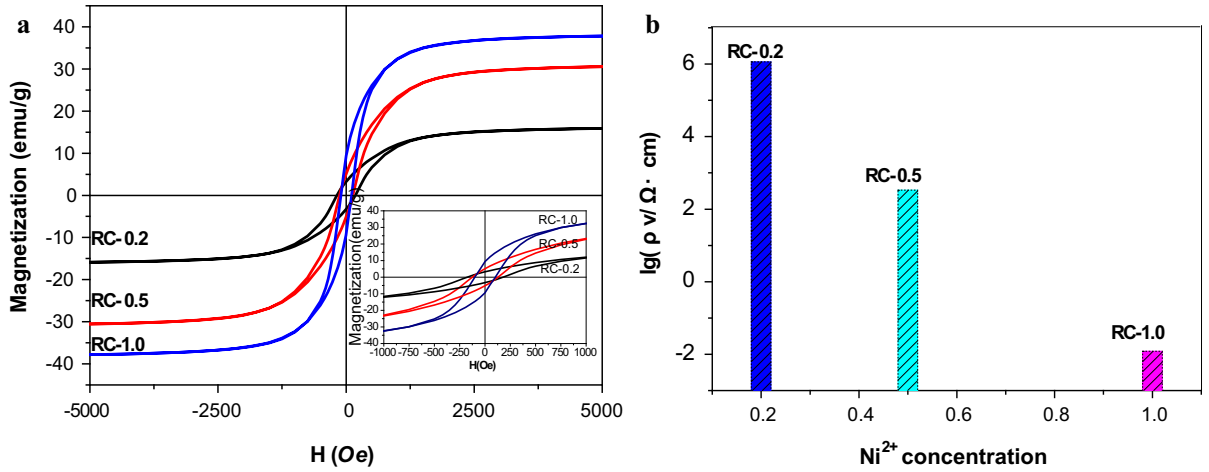

Fig. 5 The magnetic hysteresis loops (**a**) and the resistance values of nanocomposites RC-0.2, RC-0.5, and RC-1.0 at 298 K

materials, the good electrical conductivity is beneficial for use as electromagnetic shielding and energy storage textiles.

The rapid explosion of electromagnetic (EM) wave communications in industrial, commercial, and military applications has brought serious EM interference and compatibility problems. This is why advanced EM wave absorption materials have been attracting considerable attention (Sun et al. 2011). The reflection loss, *RL* (dB), is an effective evaluation standard of the microwave absorbance capacity of materials, can be used to indicate the microwave absorption properties of metal-backed slabs of material, and low reflection corresponds to high absorption. The *RL* value of −10 dB is comparable to 90 % of EM wave attenuation and can be considered an effective absorbent in practical applications. In the present study, thanks to the facile method, we can observe the absorption ability of the Ni/Cellulose nanocomposites directly by measuring their reflection loss (*RL*) value-frequency curves at 2–18 GHz.

Figure 6 shows the *RL* value-frequency curves of nanocomposite samples RC-0.2, RC-0.5 and RC-1.0 with the same thickness of 3 mm. It can be seen from the reflectivity curves that the absorption properties of as-prepared Ni/cellulose nanocomposites tend to increase regularly with increasing content of Ni nanoparticles. The reason may lie in that elevating content of the absorbent favors to enhance the energy dissipation and interaction between electromagnetic waves and absorbing materials thereby benefiting absorption capacity. Nevertheless, it should be noted

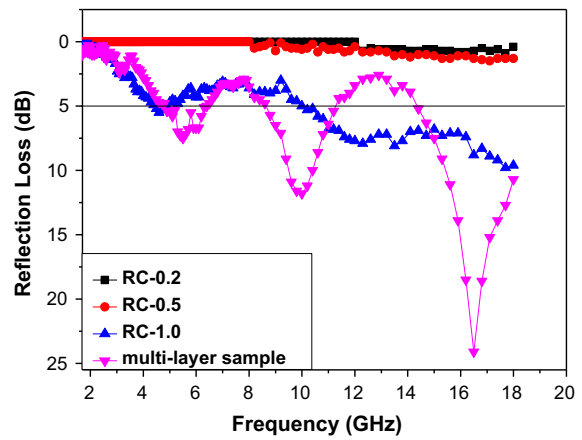

Fig. 6 *RL* curves of nanocomposite samples RC-0.2, RC-0.5 and RC-1.0 and multi-layer sample with the same thickness of 3 mm

that, although nickel as a magnetic metal is an effective absorbent, its excellent conductive properties are harmful to its absorption capacity. Namely, the higher content of nickel particles, the lower resistance of as-prepared Ni/cellulose nanocomposites will be. As a result, impedance mismatch between air and as-prepared nanocomposites will be induced to cause a strong reflection wave on the nanocomposite surface thereby setting off the incidence and absorption of electromagnetic wave (Yusoff et al. 2002).

The electromagnetic matching is highly related to the nature of fillers and can be effectively controlled by tailoring components, loading content and structures (Cao et al. 2003). To acquire desired absorption properties in selected broad range of frequency, a

multi-layer microwave absorbing material with a total thickness of 3 mm was designed. Briefly, the surface layer RC-0.2 as the matching layer exhibits little absorption capacity and allows most of the incident waves to penetrate through thereby helping to acquire good impedance matching of the absorber. Beneath the matching layer are the absorption layers RC-0.5 and RC-1.0 which play an important role in incident wave attenuation and multiple reflections associated with inhomogeneity within the absorber. As what is expected, the multi-layer sample exhibits good absorption capacity and shows three remarkable absorption peaks in the selected frequency range of 2–18 GHz as well as an additional effective bandwidth in the low-frequency region. Particularly, it exhibits an especially low *RL* value of −24.3 dB at 16.5 GHz, and its bandwidth with reflection loss below −4 dB is larger than 10 GHz, which means it is a promising candidate of novel high-performance microwave absorbing material.

Conclusions

In summary, we adopt a direct and facile synthetic strategy to successfully incorporate monodispersed Ni nanoparticles on cellulose fibers thereby affording Ni/cellulose magnetic nanocomposites. The morphology and size of Ni nanoparticles and the properties of as-prepared nanocomposites can be well controlled by adjusting the concentration of Ni^{2+} in cellulose solution reaction system. As-prepared Ni/cellulose composites exhibit desired magnetic properties and electrical conductivity which is related to the size and morphology of Ni nanoparticles as well as the composition and crystal structure of the nanocomposites. Particularly, multi-layer sample exhibits good absorption capacity and an additional effective bandwidth in the low-frequency region, showing promising potential as candidate of novel high-performance microwave absorbing material. The present approach could be of significance in developing novel high-performance cellulose material, because cellulose fibers with rough structure as well as high oxygen content and hydroxyl density can interact with electropositive transition-metal cations and act as effective nanoreactors for in situ synthesis of metal nanoparticles, and the synthetic process is economical and facile. This, hopefully, is to help to open up new practical applications for the fabrication of other inorganic materials as well as for functional cellulose nanocomposites such as magnetic paper, and conducting and energy storage textiles.

Acknowledgments This work was financially supported by the research project of the National Natural Science Foundation of China (50902045/E0213, 20971037/B0111, and 21271063) and Science and Technology Department of Henan Province (Grant No. 114300510033).

References

Breitwieser D, Moghaddam MM, Spirk S, Baghbanzadeh M, Pivec T, Fasl H, Ribitsch V, Kappe CO (2013) In situ preparation of silver nanocomposites on cellulosic fibers-microwave vs. conventional heating. Carbohydr Polym 94:677–686

Cai J, Zhang L, Zhou J, Li H, Chen H, Jin H (2004) Novel fibers prepared from cellulose in NaOH/urea aqueous solution. Macromol Rapid Commun 25:1558–1562

Cai J, Liu Y, Zhang L (2006) Dilute solution properties of cellulose in LiOH/urea aqueous system. J Polym Sci Part B Polym Phys 44:3093–3101

Cai J, Zhang L, Chang C, Cheng G, Chen X, Chu B (2007a) Hydrogen-bond-induced inclusion complex in aqueous cellulose/LiOH/urea solution at low temperature. Chem Phys Chem 8:1572–1579

Cai J, Zhang L, Zhou J, Qi H, Chen H, Kondo T, Chen X, Chu B (2007b) Multifilament fibers based on dissolution of cellulose in NaOH/urea aqueous solution: structure and properties. Adv Mater 19:821–825

Cai J, Zhang L, Liu S, Liu Y, Xu X, Chen X, Chu B, Guo X, Xu J, Cheng H (2008) Dynamic self-assembly induced rapid dissolution of cellulose at low temperatures. Macromolecules 41:9345–9351

Cao M, Qin R, Qiu C, Zhu J (2003) Matching design and mismatching analysis towards radar absorbing coatings based on conducting plate. Mater Des 24:391–396

Dong BH, Hinestroza JP (2009) Metal nanoparticles on natural cellulose fibers: electrostatic assembly and in situ synthesis. ACS Appl Mater Interfaces 1:797–803

Donia AM, Atia AA, Abouzayed FI (2012) Preparation and characterization of nano-magnetic cellulose with fast kinetic properties towards the adsorption of some metal ions. Chem Eng J 191:22–30

El-Shishtawy RM, Asiri AM, Abdelwahed NAM, Al-Otaibi MM (2011) In situ production of silver nanoparticle on cotton fabric and its antimicrobial evaluation. Cellulose 18:75–82

French AD (2014) Idealized powder diffraction patterns for cellulose polymorphs cellulose. Cellulose 21:885–896. doi:10.1007/s10570-013-0030-4

French AD, Santiago Cintrón M (2013) Cellulose polymorphy, crystallite size, and the segal crystallinity index. Cellulose 20:583–588. doi:10.1007/s10570-012-9833-y

Gong C, Duan Y, Tian J, Wu Z, Zhang Z (2008) Preparation of fine Ni particles and their shielding effectiveness for

electromagnetic interference. J Appl Polym Sci 110: 569–577
Gong C, Tian J, Zhao T, Wu Z, Zhang Z (2009) Formation of Ni chains induced by self-generated magnetic field. Mater Res Bull 44:35–40
Gong C, Tian J, Zhang J, Zhang X, Yu L, Zhang Z (2010a) Effect of processing conditions on the structure and collective magnetic properties of flowerlike nickel nanostructures. Mater Res Bull 45:682–687
Gong C, Zhang J, Zhang X, Yu L, Zhang P, Wu Z, Zhang Z (2010b) Strategy for ultrafine Ni fibers and investigation of the electromagnetic characteristics. J Phys Chem C 114:10101–10107
Gong C, Wang X, Zhang X, Zhao X, Meng H, Jia Y, Zhang J, Zhang Z (2014) Synthesis of Ni/SiO2 nanocomposites for tunable electromagnetic absorption. Mater Lett 121:81–84
He J, Kunitake T, Nakao A (2003) Facile in situ synthesis of noble metal nanoparticles in porous cellulose fibers. Chem Mater 15:4401–4406
Jean B, Heux L, Dubreuil F, Chambat G, Cousin F (2008) Non-electrostatic building of biomimetic cellulose–xyloglucan multilayers. Langmuir 25:3920–3923
Jia F, Zhang L, Shang X, Yang Y (2008) Non-aqueous sol–gel approach towards the controllable synthesis of nickel nanospheres, nanowires, and nanoflowers. Adv Mater 20: 1050–1054
Klemm D, Heublein B, Fink HP, Bohn A (2005) Cellulose: fascinating biopolymer and sustainable raw material. Angew Chem Int Ed 44:3358–3393
Kondo T, Sawatari C (1996) A Fourier transform infrared spectroscopic analysis of the character of hydrogen bonds in amorphous cellulose. Polymer 37(3):393–399
Langan P, Nishiyama Y, Chanzy H (2001) X-ray structure of mercerized cellulose II at 1 Å resolution. Biomacromolecules 2:410–416. doi:10.1021/bm005612q
Li R, Zhang L, Xu M (2012) Novel regenerated cellulose films prepared by coagulating with water: Structure and properties. Carbohydr Polym 87:95–100
Liu S, Zhou J, Zhang L, Guan J, Wang J (2006) Synthesis and alignment of iron oxide nanoparticles in a regenerated cellulose film. Macromol Rapid Commun 27:2084–2089
Liu S, Hu H, Zhou J, Zhang L (2011) Cellulose scaffolds modulated synthesis of Co_3O_4 nanocrystals: preparation, characterization and properties. Cellulose 18:1273–1283
Magalhães WLE, Cao X, Lucia LA (2009) Cellulose nanocrystals cellulose core-in-shell nanocomposite assemblies. Langmuir 22:13250–13257
Nishiyama Y, Langan P, Chanzy H (2002) Crystal structure and hydrogen-bonding system in cellulose Iβ from synchrotron X-ray and neutron fiber diffraction. J Am Chem Soc 124(31):9074–9082. doi:10.1021/ja0257319
Nishiyama Y, Johnson GP, French AD (2012) Diffraction from nonperiodic models of cellulose crystals. Cellulose 19: 319–336. doi:10.1007/s10570-012-9652-1
Qi H, Chang C, Zhang L (2008) Effects of temperature and molecular weight on dissolution of cellulose in NaOH/urea aqueous solution. Cellulose 15:779–787
Qi H, Chang C, Zhang L (2009a) Properties and applications of biodegradable transparent and photoluminescent cellulose films prepared via a green process. Green Chem 11: 177–184
Qi H, Cai J, Zhang L, Kuga S (2009b) Properties of films composed of cellulose nanowhiskers and a cellulose matrix regenerated from alkali/urea solution. Biomacromolecules 10:1597–1602
Rubacha M (2006) Magnetically active composite cellulose fibers. J Appl Polym Sci 101:1529–1534
Schwanninger M, Rodrigues JC, Pereira H, Hinterstoisser B (2004) Effects of short-time vibratory ball milling on the shape of FT-IR spectra of wood and cellulose. Vib Spectrosc 36(1):23–40
Shafi KV, Gedanken A, Prozorov R, Balogh J (1998) Sonochemical preparation and size-dependent properties of nanostructured $CoFe_2O_4$ particles. Chem Mater 10: 3445–3450
Soumare Y, Piquemal JY, Maurer T, Ott F, Chaboussant G, Falqui A, Viau G (2008) Oriented magnetic nanowires with high coercivity. J Mater Chem 18:5696–5702
Sun G, Dong B, Cao M, Wei B, Hu C (2011) Hierarchical dendrite-like magnetic materials of Fe_3O_4, γ-Fe_2O_3, and Fe with high performance of microwave absorption. Chem Mater 23:1587–1593
Wang G, Chen X, Duan Y, Liu S (2008) Electromagnetic properties of carbon black and barium titanate composite materials. J Alloys Compd 454:340–346
Wang RH, Jiang JS, Hu M (2009) Metallic cobalt microcrystals with flowerlike architectures: synthesis, growth mechanism and magnetic properties. Mater Res Bull 44:1468–1473
Wotschadlo J, Liebert T, Clement JH, Anspach N, Höppener S, Rudolph T, Müller R, Schacher FH, Schubert US, Heinze T (2013) Biocompatible multishell architecture for iron oxide nanoparticles. Macromol Biosci 13:93–105
Yang Q, Qin X, Zhang L (2011) Properties of cellulose films prepared from NaOH/urea/zincate aqueous solution at low temperature. Cellulose 18:681–688
Yu G, Hu L, Vosgueritchian M, Wang H, Xie X, McDonough JR, Cui X, Cui Y, Bao Z (2011) Solution-processed graphene/MnO_2 nanostructured textiles for high-performance electrochemical capacitors. Nano Lett 11:2905–2911
Yusoff A, Abdullah M, Ahmad S, Jusoh S, Mansor A, Hamid S (2002) Electromagnetic and absorption properties of some microwave absorbers. J Appl Phys 92:876–882
Zhang H, Wu G, Chen X, Qiu X (2006) Synthesis and magnetic properties of nickel nanocrystals. Mater Res Bull 41: 495–501
Zhou J, Li R, Liu S, Li Q, Zhang L, Zhang L, Guan J (2009) Structure and magnetic properties of regenerated cellulose/Fe_3O_4 nanocomposite films. J Appl Polym Sci 111:2477–2484